The crystal structures and quasi-one-dimensional electronic properties of $Ag_{1+x}V_3O_8$ and $Na_{1+x}V_3O_8$

2004 J. Phys.: Condens. Matter 16 8957

(http://iopscience.iop.org/0953-8984/16/49/011)

INSTITUTE OF PHYSICS PUBLISHING JOURNAL OF PHYSICS: CONDENSED MATTER

J. Phys.: Condens. Matter **16** (2004) 8957–8969 PII: S0953-8984(04)85494-8

The crystal structures and quasi-one-dimensional electronic properties of $Ag_{1+x}V_3O_8$ and $Na_{1+x}V_3O_8$

Masashige Onoda

Institute of Physics, University of Tsukuba, Tennodai, Tsukuba 305-8571, Japan

E-mail: onoda@sakura.cc.tsukuba.ac.jp

Received 27 August 2004
Published 26 November 2004
Online at stacks.iop.org/JPhysCM/16/8957
doi:10.1088/0953-8984/16/49/011

Abstract

The crystal structures of $M_{1+x}V_3O_8$, where $M_{1+x} = Ag_{1.229}$ and $Na_{1.164}$, isomorphous to the $Li_{1+x}V_3O_8$ insertion electrode have been determined with x-ray four-circle diffraction. The networks of V ions are similar to each other, but significant differences for the M–O and M–M distances exist. The present results indicate that the Li insertion for the Ag system forces the Ag–O distance to be short, which results in an irreversible charge–discharge process accompanied with a deposition reduction of Ag ions. Both the Ag and the Na system exhibit that the donated electrons reside at specific V sites, which leads to quasi-one-dimensional electronic properties along the monoclinic *b*-axis notwithstanding the complicated structure. The semiconducting transport mechanism is of variable-range hopping in one dimension and the magnetic properties are explained with a one-dimensional Heisenberg-like model.

1. Introduction

Transition metal oxides exhibit a great variety of physical and chemical phenomena. In recent years, the insertion electrode system has received considerable attention. $Li_{1+x}V_3O_8$ is one of several vanadium oxide systems that have such properties [1–4], and it can accommodate around three or four additional Li ions per formula unit (namely $x = 3$–4) [5]. From the viewpoint of basic sciences, this lithiation is considered to supply a new kind of material for the investigation of quantum-spin fluctuation and correlated electron systems, although the crystal structures are rather complicated compared with those for the well known insertion electrode systems, $LiCoO_2$ with a triangular lattice and $LiMn_2O_4$ with a spinel lattice.

The structural and electronic properties of $Li_{1+x}V_3O_8$ with $0 \leqslant x < 0.4$ were investigated by the author's group [4]. Structure refinements for single crystals with $x = 0.06$ and 0.29 reveal the preferential and partial reduction of V ions which gives rise to low-dimensional electronic properties. The composition with $x = 0$ indicates a quasi-one-dimensional

polaronic transport in the localized states of band tails due to the slight deficiency of oxygen atoms. For $x > 0.1$ with nearly stoichiometric oxygen atoms, small polarons exist without carrier-creation energy at high temperatures, while at low temperatures the conduction may be of variable-range hopping (VRH) type. For $x > 0.2$, one-dimensional magnetic properties appear due to sizable exchange couplings, and order–disorder effects of additional Li ions lead to a significant change of transport properties. For the intermediate compositions $0 < x \leqslant 0.1$, strong randomness of the Li doping and the congenital oxygen deficiency cause VRH states even at high temperatures.

Both $Ag_{1+x}V_3O_8$ and $Na_{1+x}V_3O_8$ are known to be isomorphous to the Li system [6, 7]. There are atomic parameters only for $Ag_{1+x}V_3O_8$, which suggest that x Ag atoms are located *out of* the mirror plane in contrast to the Li system [8]. The Ag and Na systems can accommodate about four and three Li ions per formula unit, respectively, although the electrochemical reaction for the former is accompanied with the reduction of Ag ions [9, 10]. There is little information on the basic physical properties for these systems.

As described above, $Li_{1+x}V_3O_8$ shows quasi-one-dimensional electronic properties due to the preferential reduction for the V ions. Similar properties may be expected for $M_{1+x}V_3O_8$ with M = Ag and Na, if the valence distributions are close to that for the Li system irrespective of the ionic radii of M. In section 2, detailed structures of the Ag and Na systems determined on the basis of x-ray four-circle diffraction measurements are described, and the anomalous occupancy of Ag ions postulated previously is rejected. In section 3, the electronic properties revealed through measurements of electrical resistivity, thermoelectric power and magnetization are discussed, referring to the structural results. Section 4 is devoted to conclusions.

2. Crystal structures

2.1. Lattice constants

Polycrystalline specimens of $Ag_{1+x}V_3O_8$ in the nominal range $0 \leqslant x \leqslant 0.4$ were prepared by the solid-state reaction method. First, V_2O_3 was made according to the procedure described in [11]. Then, vacuum-sealed mixtures of $2(1+x)Ag_2O$ (purity 99.9%), $(6-x)V_2O_5$ (99.99%) and xV_2O_3 were heated at 803 K for 24 h. Single crystals for the structure analysis were grown by sintering the polycrystals of $Ag_{1.2}V_3O_8$ repeatedly in air. Although this condition seems to be unreasonable for the preparation of reduced compounds, it is found that for $x \simeq 1.2$ of the Ag and Na systems, the desired specimen can be obtained.

For $Na_{1+x}V_3O_8$, polycrystalline specimens in the nominal range $0 \leqslant x \leqslant 0.4$ were prepared by heating vacuum-sealed mixtures of $4(1+x)NaVO_3$, $(4-3x)V_2O_5$ and xV_2O_3 at 853 K for 10 h. Here $NaVO_3$ was made by heating a mixture of Na_2CO_3 (99.99%) and V_2O_5 in air at 823 K for 48 h. Single crystals with a nominal composition of $Na_{1.2}V_3O_8$ were grown by heating a mixture of $2Na_2CO_3$ and $5V_2O_5$ in air at 823 K and by cooling it slowly.

The x-ray powder diffraction patterns were taken at room temperature using a Rigaku RAD-IIC diffractometer with Cu Kα radiation. The single phase with primitive monoclinic symmetry was confirmed for $Ag_{1+x}V_3O_8$ with $0.2 \leqslant x \leqslant 0.35$ and $Na_{1+x}V_3O_8$ with $0.1 \leqslant x \leqslant 0.35$. Figures 1(a) and (b) show the composition dependences of the lattice constants for $Ag_{1+x}V_3O_8$ and $Na_{1+x}V_3O_8$, respectively. Here the full circles indicate the results for single crystals determined by the x-ray four-circle diffraction. For $x \leqslant 0.3$, the lattice constants increase with increasing x except for c of the Ag system. In particular, a increases significantly, which means that the interlayer distance varies sensitively on doping of M. On the other hand, for the larger x, the lattice constants depend little on the composition. Since the volume V increases linearly for $x \leqslant 0.3$ and seems to saturate for the larger x, a simple Vegard's law appears to be valid in the region up to about 0.3.

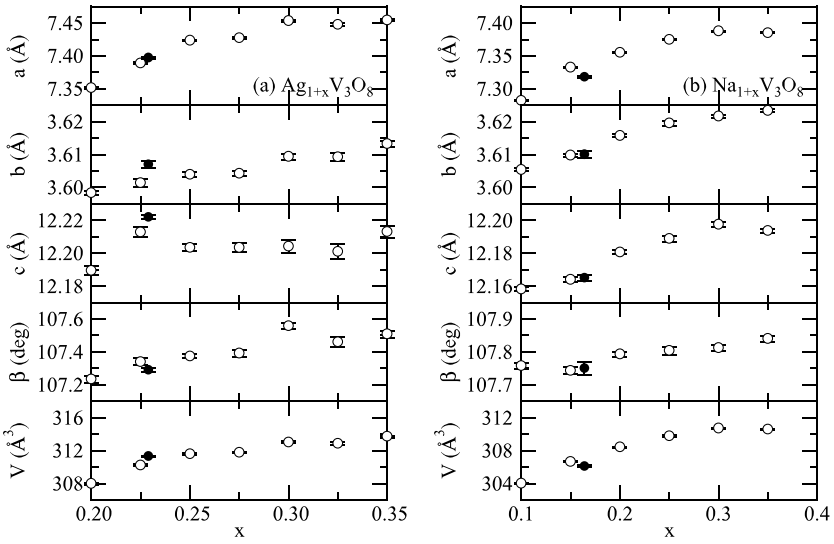

Figure 1. The composition dependences of the lattice constants for (a) $Ag_{1+x}V_3O_8$ and (b) $Na_{1+x}V_3O_8$, where open and full circles indicate the results on the basis of the x-ray powder diffraction and the four-circle diffraction, respectively.

2.2. Structure determinations

The x-ray four-circle diffraction measurements for $Ag_{1+x}V_3O_8$ and $Na_{1+x}V_3O_8$ were performed with graphite-monochromated Mo Kα radiation and an 18 kW rotating-anode generator. The crystal data and a summary of intensity measurements, structure solutions, and refinements are listed in table 1. The structures were refined successfully by full-matrix least-squares calculations with anisotropic displacement parameters on the basis of atomic parameters for $Li_{1+x}V_3O_8$ described in [4]. Here the atomic scattering factors were taken from [12], and anomalous dispersion effects were included with the values given by [13]. All of the calculations were performed using the teXsan crystallographic software package [14].

The structural frameworks refined here[1] essentially correspond to the previous one [4]. The atomic coordinates, equivalent isotropic thermal parameters, and anisotropic displacement parameters determined with the same atomic labelling scheme as that for $Li_{1+x}V_3O_8$ [4] are listed in table 2. Selected interatomic distances are listed in table 3 with the previous result for the Li system. The crystal structure projected on the *ac*-plane of $Ag_{1.229}V_3O_8$ is shown in figure 2(a), where the open and shaded circles denote positions at $y = 1/4$ and $3/4$, respectively. There exist three crystallographically independent V sites labelled V1, V2 and V3. The V1 ions have a pyramidal coordination, while the V2 and V3 ions have octahedral coordinations. The chains of VO_6 octahedra and those of VO_5 pyramids extending along the *b*-axis are linked by corner-shared oxygens to form continuous sheets of V–O polyhedra; that is, a V_3O_8 framework. As pointed out in [4], the networks for the equivalent sites of V1 and V2 are expressed as zigzag chains and that for the V3 site is a one-dimensional chain. The M ions reside in an octahedral site (M1) with a full occupancy and the excess xM ions are in a tetrahedral site (M2) with a probability of 0.229(1) for M = Ag and 0.164(4) for M = Na as shown in figure 2(b). The M2 sites with M2–M2 distances listed in table 3 as indicated by the dashed line cannot be occupied simultaneously due to the strong Coulomb repulsion.

[1] Supplementary data files are available from the article's abstract page in the online journal; see http://www.iop.org.

Table 1. Crystal data and summary of intensity measurements, structure solutions, and refinements of $Ag_{1.229}V_3O_8$ and $Na_{1.164}V_3O_8$.

	$Ag_{1.229}V_3O_8$	$Na_{1.164}V_3O_8$
Crystal dimensions (mm)	$0.42 \times 0.11 \times 0.02$	$0.30 \times 0.09 \times 0.01$
Temperature (K)	295	297
Crystal system	Monoclinic	Monoclinic
Space group	$P2_1/m$	$P2_1/m$
Z value	2	2
a (Å)	7.397(2)	7.318(2)
b (Å)	3.607(1)	3.610(1)
c (Å)	12.222(1)	12.165(2)
β (deg)	107.29(1)	107.75(2)
V (Å^3)	311.3(1)	306.1(1)
Diffractometer	Rigaku AFC-7R	Rigaku AFC-7R
Radiation	Mo Kα	Mo Kα
$2\theta_{max}$ (deg)	90	80
Number of unique reflections	2855	2122
R_{int}	0.025	0.043
Corrections	Lorentz-polarization Absorption (trans 0.4818–0.8781) Secondary extinction	Lorentz-polarization Absorption (trans 0.7727–1) Secondary extinction
Structure solution	Parameters in [4]	Parameters in [4]
Least-squares refinement	Full-matrix	Full-matrix
Number of observations	2146 ($F > 3\sigma$)	1527 ($F > 3\sigma$)
Number of variables	81	81
R-factor[a]	0.023	0.024
R_w-factor[b]	0.025	0.029
Structure analysis	teXsan	teXsan

[a] $R = \left[\sum (|F_o| - |F_c|)^2\right] / \left(\sum |F_o|\right)$.

[b] $R_w = \left\{\left[\sum w (|F_o| - |F_c|)^2\right] / \left(\sum w F_o^2\right)\right\}^{1/2}$.

Therefore, for M1 and M2 sites alone, the composition of $M_{1+x}V_3O_8$ is limited to $x = 0.5$. Of $M_{1+x}V_3O_8$ compounds, the Ag system is found to be most unstable energetically due to the short Ag2–Ag2 distance. The recent structure determination for $Ag_{1.2}V_3O_8$ has suggested that 0.2Ag atoms are located out of the mirror plane [8], but this work with significantly better R- and R_w-factors (see table 1) reveals that no such an anomaly exists there; that is, M2 ions are located on the mirror plane. The compositions for the Ag and Na systems are expressed as $Ag_{1.229}V_3O_8$ and $Na_{1.164}V_3O_8$, respectively, nearly corresponding to the nominal values $x = 1.2$. On the basis of the average distances of M1–O and M2–O listed in table 3, the ionic radii of M1 and M2 for M = Ag are estimated to be 1.06 and 0.93 Å, respectively, and those for M = Na are 1.04 and 0.87 Å taking 1.38 Å as an effective radius of O^{2-}. According to [15], the ionic radii of Ag^+ (Na^+) with octahedral and tetrahedral environments are 1.15 (1.02) and 1.00 (0.99) Å, respectively. Therefore, the ionic radii of M are found to be responsible for the M–O distances.

On the basis of the bond-length–bond-strength relation [16], the effective valences of V ions are estimated as listed in table 3. The average V valences expected from the chemical formula $Ag_{1.229}V_3O_8$ and $Na_{1.164}V_3O_8$ are 4.92 and 4.94, respectively, which agree roughly with the average values for each effective valence. As in the case of the Li system, the V1 ion is considered to be nearly pentavalent, and the V3 ion is in a mixed valent state of V^{4+} and V^{5+}. The V2 ion is also likely to be in the mixed valent state, which is contrary to the case of $Li_{1.29}V_3O_8$,

Table 2. Atomic coordinates, equivalent isotropic thermal parameters B_{eq} (Å^2) and anisotropic displacement parameters U_{ij} of $Ag_{1.229}V_3O_8$ at 295 K and those of $Na_{1.164}V_3O_8$ at 297 K, where $y = 1/4$ and $U_{12} = U_{23} = 0$ for all of the atoms. B_{eq} and U_{ij} are defined by $B_{eq} = \frac{8}{3}\pi^2[U_{11}(aa^*)^2 + U_{22}(bb^*)^2 + U_{33}(cc^*)^2 + 2U_{12}aa^*bb^*\cos\gamma + 2U_{13}aa^*cc^*\cos\beta + 2U_{23}bb^*cc^*\cos\alpha]$, and the parameters are defined in the thermal factor form $T = \exp[-2\pi^2(a^{*2}U_{11}h^2 + b^{*2}U_{22}k^2 + c^{*2}U_{33}l^2 + 2a^*b^*U_{12}hk + 2a^*c^*U_{13}hl + 2b^*c^*U_{23}kl)]$. For Ag2 and Na2, the occupancy probabilities are 0.229(1) and 0.164(4), respectively.

Atom	x	z	B_{eq}	U_{11}	U_{22}	U_{33}	U_{13}
			For $Ag_{1.229}V_3O_8$				
V1	0.862 20(5)	0.540 55(3)	0.738(5)	0.014 5(1)	0.006 5(1)	0.007 8(1)	0.004 47(10)
V2	0.181 52(6)	0.078 19(3)	1.045(5)	0.021 3(2)	0.006 9(1)	0.009 2(1)	0.001 0(1)
V3	0.069 67(6)	0.807 40(3)	1.034(5)	0.022 7(2)	0.008 5(1)	0.009 0(1)	0.006 1(1)
O1	0.060 1(3)	0.460 3(1)	1.00(2)	0.019 9(7)	0.006 4(5)	0.014 6(6)	0.009 3(5)
O2	0.895 1(3)	0.929 0(1)	1.14(3)	0.024 0(8)	0.006 7(5)	0.011 3(6)	0.003 2(5)
O3	0.832 6(3)	0.674 9(1)	1.03(2)	0.020 3(7)	0.010 8(6)	0.009 0(5)	0.005 9(5)
O4	0.377 8(3)	0.182 9(1)	1.52(3)	0.024 0(9)	0.016 3(8)	0.013 3(6)	−0.001 0(6)
O5	0.649 4(3)	0.450 9(1)	1.33(3)	0.018 3(7)	0.015 6(7)	0.014 1(6)	0.000 9(5)
O6	0.258 2(3)	0.956 1(1)	1.37(3)	0.023 8(8)	0.016 6(7)	0.010 8(6)	0.003 5(5)
O7	0.212 2(3)	0.730 9(2)	1.62(3)	0.023 1(9)	0.023 8(9)	0.016 6(7)	0.008 6(6)
O8	0.985 5(3)	0.173 3(1)	1.19(3)	0.026 3(8)	0.008 2(6)	0.010 4(5)	0.005 0(5)
Ag1	0.505 32(3)	0.678 03(2)	1.566(3)	0.019 53(8)	0.018 02(8)	0.019 95(8)	0.002 81(6)
Ag2	0.553 1(2)	0.020 1(1)	3.77(3)	0.019 8(5)	0.049 7(9)	0.076 (1)	0.017 4(6)
			For $Na_{1.164}V_3O_8$				
V1	0.861 48(6)	0.541 15(4)	0.600(6)	0.009 8(2)	0.006 6(2)	0.007 0(1)	0.003 5(1)
V2	0.184 11(7)	0.080 24(4)	0.778(6)	0.013 4(2)	0.006 7(2)	0.008 1(2)	0.001 3(1)
V3	0.078 68(7)	0.810 83(4)	0.894(7)	0.016 3(2)	0.010 0(2)	0.008 9(2)	0.005 5(2)
O1	0.061 0(3)	0.460 4(2)	0.88(3)	0.017 0(8)	0.005 5(7)	0.013 8(8)	0.009 1(7)
O2	0.894 8(3)	0.927 3(2)	0.87(3)	0.016 1(8)	0.007 6(7)	0.009 2(7)	0.003 6(6)
O3	0.837 3(3)	0.676 6(2)	0.82(3)	0.014 2(8)	0.010 6(8)	0.007 2(7)	0.004 4(6)
O4	0.378 0(3)	0.188 9(2)	1.20(3)	0.017 5(9)	0.015 7(9)	0.009 4(7)	−0.000 6(7)
O5	0.644 1(3)	0.453 3(2)	1.23(3)	0.012 2(8)	0.018 2(10)	0.013 7(8)	0.000 0(7)
O6	0.267 1(3)	0.961 3(2)	1.02(3)	0.015 7(8)	0.014 3(9)	0.008 1(7)	0.002 6(6)
O7	0.223 7(3)	0.735 6(2)	1.34(4)	0.017 4(9)	0.022(1)	0.014 1(8)	0.008 0(8)
O8	0.976 1(3)	0.171 9(2)	0.94(3)	0.018 4(8)	0.008 7(7)	0.008 5(7)	0.004 1(7)
Na1	0.508 5(2)	0.674 5(1)	1.47(2)	0.016 0(6)	0.017 5(6)	0.021 5(6)	0.004 1(5)
Na2	0.568 (1)	0.059 3(9)	2.1(2)	0.017 (4)	0.021 (4)	0.048 (6)	0.018 (4)

although the electron density is rather smaller than that for V3. This result suggests that, for the Ag and Na systems, the V3 ion is mainly responsible for the transport and magnetic properties, but the V2 chain also partially contributes to them. A clinographic view for the network of the V2 and V3 ions is shown in figure 2(c). Using the Hartree–Fock function for V^{4+} [17], the ground-state wavefunctions in the $V1O_6$, $V2O_6$ and $V3O_6$ octahedra for $Ag_{1.229}V_3O_8$ are calculated to be $-0.793d_{yz} + 0.608d_{xy}$, $-0.999d_{yz} - 0.035d_{xy}$ and $-0.995d_{xy} + 0.094d_{yz}$, respectively; and those for $Na_{1.164}V_3O_8$ are $0.775d_{yz} - 0.631d_{xy}$, $-0.995d_{yz} - 0.091d_{xy}$ and $0.991d_{xy} - 0.127d_{yz}$, where $\boldsymbol{x} \parallel 2\boldsymbol{a} + \boldsymbol{c}$, $\boldsymbol{y} \parallel -\boldsymbol{b}$ and $\boldsymbol{z} \parallel \boldsymbol{x} \times \boldsymbol{y}$. The effective valences and wavefunctions of V ions for $Ag_{1+x}V_3O_8$ and $Na_{1+x}V_3O_8$ described above indicate the electronic transports to be one-dimensional, since the V3 and V2 chains reduced partially are separated by the closed-shell ions of V^{5+} and M^+ in the ac-plane. The magnetic interactions are also expected to be one-dimensional, since the superexchange couplings through the corner-shared paths along the b-axis are considered most effective based on a qualitative rule [18].

Table 3. Selected V–O, M–O and M–M distances (Å); V valences and wavefunctions; and V–V distances and V–O–V angles (deg) of the exchange paths for V2 and V3 of $M_{1+x}V_3O_8$, where the symmetry operators are (i) x, y, z; (ii) $1-x, -\frac{1}{2}+y, 1-z$; (iii) $1-x, \frac{1}{2}+y, 1-z$; (iv) $1+x, y, z$; (v) $-1+x, y, -1+z$; (vi) $x, y, -1+z$; (vii) $-1+x, y, z$; (viii) $1-x, -\frac{1}{2}+y, -z$; (ix) $1-x, \frac{1}{2}+y, -z$; (x) $x, -1+y, z$; (xi) $x, 1+y, z$; (xii) $-x, \frac{1}{2}+y, -z$; (xiii) $-x, -\frac{1}{2}+y, -z$; (xiv) $1+x, y, 1+z$; (xv) $-x, -\frac{1}{2}+y, 1-z$; (xvi) $-x, \frac{1}{2}+y, 1-z$; (xvii) $x, y, 1+z$.

	$Li_{1.29}V_3O_8$ [4]	$Ag_{1.229}V_3O_8$	$Na_{1.164}V_3O_8$
$V1O_6$ octahedra[a]			
V1(i)–O1(ii, iii)	1.896(2)	1.8937(7)	1.894(1)
V1(i)–O1(iv)	1.980(2)	1.989(2)	1.992(2)
V1(i)–O3(i)	1.738(2)	1.720(2)	1.711(2)
V1(i)–O5(i)	1.615(3)	1.629(2)	1.624(2)
V1(i)–O7(iv)	2.831(3)	2.921(2)	2.966(2)
V1 valence	4.93(2)	4.91(1)	4.96(1)
Wavefunction	$0.898d_{yz}$	$-0.793d_{yz}$	$0.775d_{yz}$
	$-0.439d_{xy}$	$+0.608d_{xy}$	$-0.631d_{xy}$
$V2O_6$ octahedra			
V2(i)–O2(v)	2.336(2)	2.349(2)	2.354(2)
V2(i)–O2(ii, iii)	1.885(2)	1.884 4(7)	1.889(1)
V2(i)–O4(i)	1.613(2)	1.625(2)	1.618(2)
V2(i)–O6(vi)	1.742(2)	1.747(2)	1.732(2)
V2(i)–O8(vii)	2.103(2)	2.111(2)	2.144(2)
V2 valence	4.94(1)	4.85(1)	4.88(1)
Wavefunction	$0.999d_{yz}$	$-0.999d_{yz}$	$-0.995d_{yz}$
	$-0.023d_{xy}$	$-0.035d_{xy}$	$-0.091d_{xy}$
$V3O_6$ octahedra			
V3(i)–O2(vii)	2.217(2)	2.240(2)	2.232(2)
V3(i)–O3(vii)	1.998(2)	2.002(2)	2.007(2)
V3(i)–O6(i)	1.974(2)	1.934(2)	1.927(2)
V3(i)–O7(i)	1.607(2)	1.604(2)	1.599(2)
V3(i)–O8(ii, iii)	1.874(2)	1.8791(7)	1.874(1)
V3 valence	4.66(1)	4.70(1)	4.76(1)
Wavefunction	$0.999d_{xy}$	$-0.995d_{xy}$	$0.991d_{xy}$
	$-0.038d_{yz}$	$+0.094d_{yz}$	$-0.127d_{yz}$
$M1O_6$ octahedra			
M1(i)–O3(i)	2.044(8)	2.432(2)	2.398(2)
M1(i)–O4(ii, iii)	2.358(6)	2.452(1)	2.422(2)
M1(i)–O5(ii, iii)	2.294(6)	2.444(1)	2.422(2)
M1(i)–O7(i)	2.051(8)	2.439(2)	2.417(2)
M1–O average	2.233	2.443	2.417
$M2O_4$ tetrahedra			
M2(i)–O4(i)	2.30(2)	2.679(2)	2.401(9)
M2(i)–O6(vi)	1.90(2)	2.087(2)	2.163(9)
M2(i)–O6(ii, iii)	2.01(1)	2.245(1)	2.226(5)
M2–O average	2.055	2.314	2.254
M2(i)–M2(viii, ix)	2.17(3)	1.970(1)	2.34(1)
Exchange paths for V2 and V3			
V2(i)–V2(x, xi)	3.607(3)	3.607(1)	3.610(2)
V2(ii)–O2(i)–V2(iii)	146.1(1)	146.3(1)	145.7(1)
V2(i)–V2(xii, xiii)	3.318(2)	3.3264(9)	3.335(1)
V2(iii)–O2(i)–V2(xiv)	103.09(7)	103.03(5)	103.10(6)
V2(i)–V3(xv, xvi)	3.174(1)	3.1942(7)	3.2040(9)
V2(iii)–O2(i)–V3(iv)	101.09(7)	101.17(5)	101.75(6)
V2(iv)–O8(i)–V3(iii)	105.78(7)	106.22(5)	105.55(6)

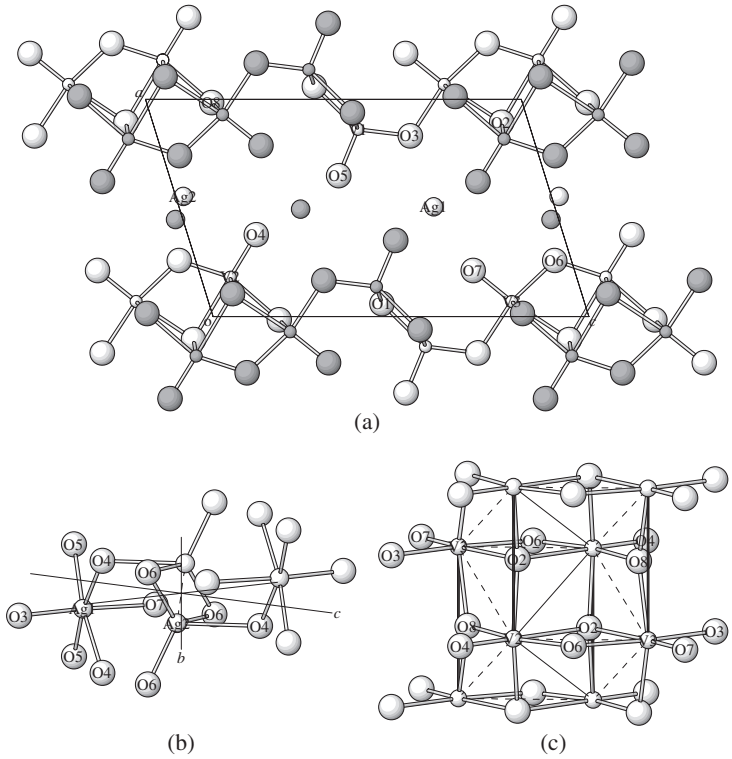

Figure 2. The crystal structure of $Ag_{1.229}V_3O_8$ at 295 K: (a) the projection on the monoclinic *ac*-plane, where the open and shaded circles denote positions at $y = 1/4$ and $3/4$, respectively; (b) the clinographic view for the environment of Ag1 and Ag2 ions, where the dashed line shows the symmetry-related Ag2–Ag2 pair; and (c) the network of V2 and V3 ions, where the full lines and the dashed ones indicate the paths between the equivalent sites and those between the inequivalent sites, respectively, and the thin (thick) lines are for the edge-(corner)-shared paths.

Table 3. (Continued.)

	$Li_{1.29}V_3O_8$ [4]	$Ag_{1.229}V_3O_8$	$Na_{1.164}V_3O_8$
V2(i)–V3(vi)	3.1584(7)	3.1639(5)	3.1297(6)
V2(xiv)–O2(i)–V3(iv)	87.81(9)	87.14(7)	86.03(7)
V2(xvii)–O6(i)–V3(i)	116.3(1)	118.4(1)	117.5(1)
V3(i)–V3(x, xi)	3.607(3)	3.607(1)	3.610(2)
V3(ii)–O8(i)–V3(iii)	148.4(1)	147.3(1)	148.7(1)

[a] A long V–O distance is added.

3. Electronic properties

3.1. Transport properties

The electrical resistivities ρ for $Ag_{1+x}V_3O_8$ and $Na_{1+x}V_3O_8$ were measured by a dc four-terminal method at temperatures between 100 and 300 K. Here the specimens are polycrystalline except $Na_{1.164}V_3O_8$ for which the resistivity along the *b*-axis is obtained. Figure 3 shows the temperature dependences of ρ, which nearly follow VRH of the form

$$\rho = \rho_0 \exp\sqrt{\frac{T_0}{T}}, \tag{1}$$

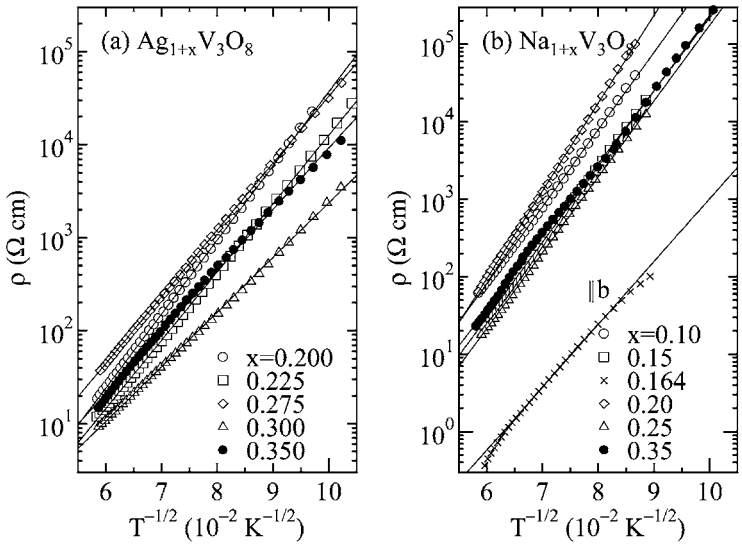

Figure 3. The temperature dependences of the electrical resistivities for (a) $Ag_{1+x}V_3O_8$ and (b) $Na_{1+x}V_3O_8$. Here the specimens are polycrystalline except $Na_{1.164}V_3O_8$, for which the resistivity along the *b*-axis is plotted. The full lines show fits to equation (1).

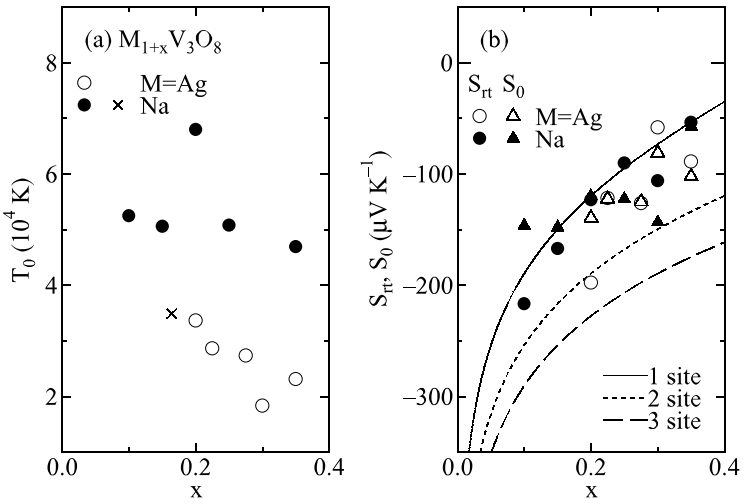

Figure 4. The composition dependences of (a) the energy gaps T_0 in equation (1) and (b) the thermoelectric powers at room temperature (S_{rt}) and at the high-temperature limit (S_0) for the polycrystalline specimens of $Ag_{1+x}V_3O_8$ and $Na_{1+x}V_3O_8$, where the cross in (a) indicates the result for single crystals of $Na_{1.164}V_3O_8$ and the curves in (b) are drawn on the basis of equation (3).

where ρ_0 is a constant. The full lines in figure 3 provide the composition dependences of T_0 shown in figure 4(a). The hopping exponent in equation (1) suggests that the transport mechanism is either Efros–Shklovskii type [19] or Mott type [20]. The former is a VRH with a soft Coulomb gap due to Coulomb interactions between the localized electrons. The latter type is that for a quasi-one-dimensional system with weak transverse coupling between the chains [21] or with a finite chain length [22, 23]. Since there is no direct evidence for a

Coulomb gap for this system, it is difficult to judge which mechanism is appropriate on the basis of the present results alone. Although almost all of the specimens considered here are polycrystalline with a possible grain-boundary resistance, their temperature dependences are similar to that of the $Na_{1.164}V_3O_8$ single crystals, suggesting that the values of T_0 in figure 4(a) are intrinsic and that they do not have a significant anisotropy. In addition, the resistivity of the single crystals is two orders of magnitude smaller than those of the polycrystals with a similar composition, which implies that the most conducting direction corresponds to the *b*-axis, as postulated from the structural viewpoint.

Considering that $Li_{1+x}V_3O_8$ exhibits the Mott-type VRH in three dimensions due to the randomness at the M2 site and/or the oxygen deficiency [4], it may be natural to think of the VRH model proposed in [21], since this model provides the temperature dependence of $\ln \rho \propto T^{1/2}$ or $T^{1/4}$ depending on the temperature range. In this case, the *interchain* hopping is considered to be responsible for the temperature dependence of ρ, and T_0 in equation (1) is given by $T_0 \approx \frac{\alpha}{n}$, where α^{-1} is the localization length and n is the one-dimensional density of states along the chain. Here it is noted that the *intrachain* VRH resistivity without any interchain coupling provides the activation-type temperature dependence which is the same as that for a single infinite chain [21, 24]. The result of T_0 shown in figure 4(a) which roughly tends to decrease with increasing x may be related to the increase of the effective density of states and/or the localization length. As mentioned above, this model leads to the weaker (three-dimensional) temperature dependence below $T^* \approx T_0/[\ln(T_0/t_\perp)]^2$, $t_\perp$ being the bandwidth in the transverse direction [21]. A difference between the hopping exponents for the Li system and the present systems suggests that $t_\perp$ for the former is relatively large; for example, when $T_0 = 10^4$ and $t_\perp = 10^1$ K, one obtains $T^* \approx 210$ K. This is consistent with the interlayer distance for $M_{1+x}V_3O_8$ decreasing on decreasing the ionic radii of M.

The thermoelectric powers S for the polycrystalline specimens of $Ag_{1+x}V_3O_8$ and $Na_{1+x}V_3O_8$ measured with a dc method at temperatures between 100 and 300 K are shown against the inverse temperature in figures 5(a) and (b), respectively. At high temperatures, all of the data have a negative sign, which suggests an electron carrier conduction, and they depend weakly on temperature. Generally the thermoelectric power for hopping conduction is expressed as

$$S \simeq \frac{w^2}{Te} \frac{\Delta \ln \sigma(\epsilon_F)}{\Delta \epsilon_F}, \tag{2}$$

where w is the hopping energy, $\sigma(\epsilon_F)$ is the electric conductivity at the Fermi energy ϵ_F and e is the electron charge [25]. For the interchain hopping in quasi-one-dimensional VRH, S may be constant, since $w \propto \sqrt{T_0 T}$, and for the intrachain hopping, $w \propto T_0$ and $S \propto 1/T$. Therefore the temperature dependence of the thermoelectric power may be approximated by the equation $S = S_0 + E_S/T$. Applications of this equation to the data at high temperatures provide results of $E_S \approx -2 \times 10^2$ K for $Ag_{1.2}V_3O_8$ and $Na_{1.1}V_3O_8$ from the full lines in figure 5. Except for these compositions, the absolute value of E_S ranges from 10^0 to 10^1 K and its sign changes from negative to positive with increasing x, which should be ascribed to the change of the energy derivative in equation (2). The composition dependences of the room temperature value S_{rt} and the high-temperature limit one S_0 are shown in figure 4(b) by the circles and triangles, respectively. S_0 is not so different from S_{rt}. A two-channel model with a parallel current path in extended and localized states at the band edges, basically applied to the transport properties of LiV_3O_8 [4], would also account for the above properties, in particular for the results of $Ag_{1.2}V_3O_8$ and $Na_{1.1}V_3O_8$. However, it is necessary to perform another experiment in order to deduce definite physical quantities for that model.

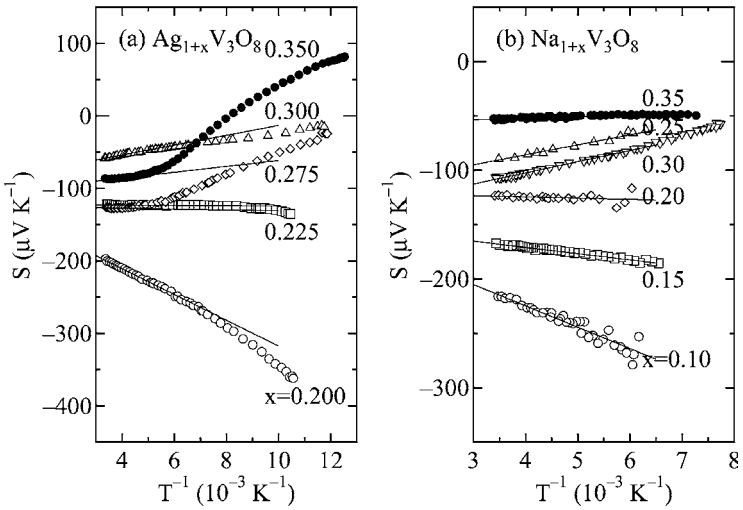

Figure 5. The temperature dependences of the thermoelectric powers for the polycrystalline specimens of (a) $Ag_{1+x}V_3O_8$ and (b) $Na_{1+x}V_3O_8$, where the full lines indicate fits to an equation $S = S_0 + E_S/T$.

The values of $S_{0,\mathrm{rt}}$ do not depend on M but on x alone. They decrease with increasing x. Let us consider the composition dependences of $S_{0,\mathrm{rt}}$ with the Heikes formula for the nondegenerate gas [26],

$$S_{\mathrm{H}} = \frac{k}{e} \ln\left(\frac{x}{N-x}\right), \tag{3}$$

where k is the Boltzmann coefficient and N is the number of V sites for the hopping, since the VRH state may be less significant in the high-temperature limit. The effective valence distributions for $Ag_{1.229}V_3O_8$ and $Na_{1.164}V_3O_8$ revealed by the previous section indicate that for both of the systems, many of the donated electrons reside at the V3 sites and a few of them are located at V2. Therefore $N = 1$ or 2 should be applied in equation (3), and the calculated results for $N = 1$–3 are shown in figure 4(b) by the full, dotted and dashed curves, respectively. A good agreement is obtained for $N = 1$, which indicates that the valence distributions for both of the systems are scaled by the number of donated electrons. It is important to point out that, for the present system, the thermoelectric powers for the nondegenerate gas (or small polaron model) are close to the values in the VRH regime.

The temperature dependences of the thermoelectric powers for $Ag_{1.275}V_3O_8$ and $Ag_{1.35}V_3O_8$ change significantly at about 200 K. The result for $Ag_{1.3}V_3O_8$ also indicates a weak anomaly at a similar temperature. This is attributed to the order–disorder effect of Ag ions with a close Ag2–Ag2 distance (1.970(1) Å for $x = 0.229$) in the regime that the VRH transport dominates on the analogy of considerations for $Li_{1+x}V_3O_8$ [4]. Such an effect is less significant for $Na_{1+x}V_3O_8$, since the Na2–Na2 distance is 2.34(1) Å for $x = 0.164$, and this is larger than those of Ag2–Ag2 and Li2–Li2 (2.17(3) Å for $x = 0.29$ [4]).

3.2. Magnetic properties

The magnetizations for the polycrystalline specimens of $Ag_{1+x}V_3O_8$ and $Na_{1+x}V_3O_8$ were measured by the Faraday method with a field of up to 1 T between 4.2 and 300 K. Both cooling

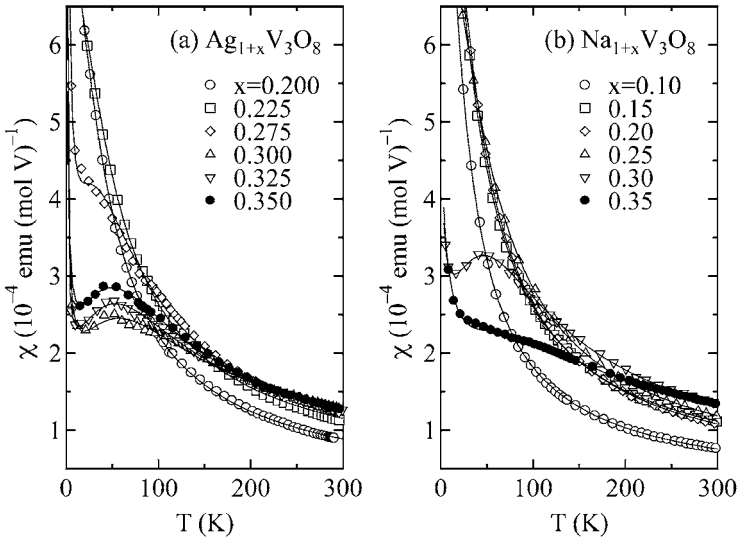

Figure 6. The temperature dependences of the magnetic susceptibilities for the polycrystalline specimens of (a) $Ag_{1+x}V_3O_8$ and (b) $Na_{1+x}V_3O_8$, where the full curves are fits to equation (4).

and heating processes were examined. The magnetic susceptibility χ was deduced from the linear part of the magnetization–field curve with a decreasing field.

Figures 6(a) and (b) show the temperature dependences of χ for $Ag_{1+x}V_3O_8$ and $Na_{1+x}V_3O_8$, respectively, where the results for the cooling and heating processes are the same within experimental accuracy. For both of the systems with $x > 0.25$, the susceptibilities exhibit a round maximum or its sign at low temperatures, while for $x \leqslant 0.25$, they indicate a Curie–Weiss law-like behaviour. The former property is a characteristic for the one-dimensional Hubbard model [27] or for the Heisenberg model with $W \ll U$, W and U being the bandwidth and the Coulomb repulsion energy, respectively [28], taking account of the structural and transport properties described above. This is caused by the significant exchange interaction between 3d spins for the preferentially reduced V ions; that is, the superexchange couplings through the corner-shared paths along the b-axis as shown in figure 2(c). A Curie-like tail at the lowest temperatures may come from a phase such as an inevitable lattice imperfection or a magnetic impurity. The results for $x \leqslant 0.25$ should also be considered with this idea, since the reduction of exchange coupling with a decrease of x and the extrinsic Curie tail may mask a round maximum of the susceptibility. Thus, the susceptibilities for all of the compositions are described in the form

$$\chi = \chi_{1D} + \chi_{isolate} + \chi_0, \tag{4}$$

where χ_{1D} is the susceptibility for an $S = \frac{1}{2}$ chain system with the parameters of the Curie constant C_{1D} and the exchange coupling[2] J_{1D} [28], $\chi_{isolate}$ is the Curie–Weiss-type susceptibility of the isolated V^{4+} ions with $C_{isolate}$ and $T_W^{isolate}$, and χ_0 corresponds to the temperature-independent susceptibility of the Van Vleck orbital and diamagnetic components. The full curves from equation (4) in figures 6(a) and (b) provide the parameters plotted in figure 7.

The composition dependences of C_{1D} shown in figure 7(a) almost follow $C_{1D} = 0.36x$ emu K mol^{-1} (full line), which indicates that x unpaired electrons donated with the Ag or Na ion have an average g-factor of 1.96. This g-factor agrees well with the value estimated from

[2] The Heisenberg Hamiltonian is defined as $H = \sum_{\langle i,j \rangle} J\boldsymbol{S}_i \cdot \boldsymbol{S}_j$, $\boldsymbol{S}_i$ being the spin operator at site i.

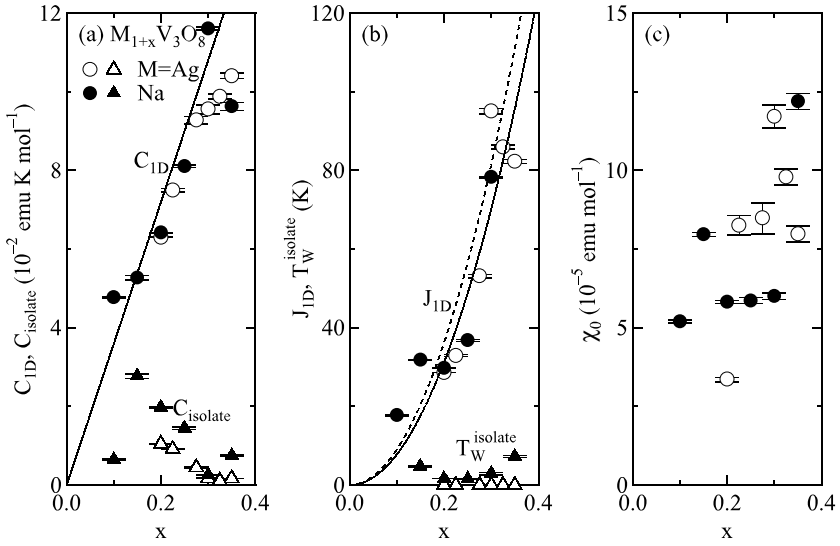

Figure 7. The composition dependences of the parameters in equation (4): (a) the Curie constants C_{1D} and $C_{isolate}$, where the full line indicates $C_{1D} = 0.36x$; (b) the exchange-coupling constants J_{1D} and the Weiss temperatures $T_W^{isolate}$, where the full (dashed) curves for $Ag(Na)_{1+x}V_3O_8$ are drawn with $J_{1D} \simeq 780\ (910)x^2$, respectively; and (c) the constant susceptibilities χ_0.

an electron paramagnetic resonance that indicates Lorentzian lineshape and nearly uniaxial symmetry for the g-factor and the linewidth [29]. Thus the application of a Heisenberg model with $W \ll U$ is justified. The results of J_{1D} for the Ag (Na) systems in figure 7(b) are expressed by the formula $J_{1D} \simeq 780(910)x^2$, as shown by the full (dotted) curves, respectively. This x dependence is easily understood with the molecular field approximation, when the d electrons are localized at a specified site. Note that the analysis for $Li_{1+x}V_3O_8$ with electron occupancy at the V3 site alone provides $J_{1D} \simeq 530x^2$ [4], which is smaller than the present results. This may be due to the small occupancy of spins at the V2 site which, as shown in figure 2(c), leads to the edge-shared exchange couplings J_e for the V2–V3 (dashed lines) as well as V2–V2 (thin lines) paths, since the V–V distances and V–O–V angles responsible for the superexchange coupling do not depend significantly on the kind of M as listed in table 3. The present results reveal the net J_e to be antiferromagnetic. The values of χ_0 shown in figure 7(c) are similar to those of $Li_{1+x}V_3O_8$ [4] and they are in a normal range as compared with those for V^{4+} with similar oxygen coordinations [30]. The results of $C_{isolate}$ and $T_W^{isolate}$ may also be reasonable for the impurity spins.

4. Conclusions

The crystal structures of $Ag_{1+x}V_3O_8$ ($x = 0.229$) and $Na_{1+x}V_3O_8$ ($x = 0.164$) with respective single-phase regions of $0.2 \leqslant x \leqslant 0.35$ and $0.1 \leqslant x \leqslant 0.35$ are determined in detail. Both of the systems exhibit that most of the donated electrons are located at the V3 site and the rest of them reside at the V2 site, leading to quasi-one-dimensional electronic properties. A significant difference between the crystal structures of $M_{1+x}V_3O_8$ with M = Li, Na and Ag is seen for the M–O and M–M distances. The former difference is attributed to that of the ionic radii of M. The M–M distance for the Ag system is very short, suggesting that it is the most unstable of these systems. The irreversible property for the charge–discharge process in

$Ag_{1+x}V_3O_8$ accompanied with a deposition reduction of Ag ions is found to be attributed to the difference of Li and Ag ionic radii; that is, the Li insertion for the Ag system forces the Ag–O distance to be short.

The transport properties are explained qualitatively in terms of the VRH-type mechanism in one dimension caused by the randomness of the M2 site. The thermoelectric power at the high-temperature limit has a composition dependence expected from a nondegenerate gas (or small polaron model). The anomaly at low temperatures in $Ag_{1+x}V_3O_8$ with $x \geqslant 0.275$ may be due to the ionic order–disorder effect for the Ag2 site. For the Na system, the Na2–Na2 distance is not so short compared with those for the Li and Ag systems, and thus no significant anomaly exists there. For all of the compositions, the magnetic properties are interpreted with a one-dimensional Heisenberg-like model, where the exchange coupling constants J_{1D} vary as x^2. The magnitudes of J_{1D} for the Ag and Na systems are significantly larger than that of the Li system. This may be due to the non-negligible occupancy of spins at the V2 site which leads to the exchange couplings for the V2–V3 edge-shared path as well as the V2–V2 zigzag-chain path.

Acknowledgments

I thank A Oyadomari and T Banno for their help with the experiments.

References

[1] Pistoia G, Pasquali M, Tocci M, Moshtev R V and Maner V 1985 *J. Electrochem. Soc.* **132** 281
[2] Kishi T, Kawakita J and Miura T 2000 *Electrochemistry* **68** 2
[3] Onoda M and Kanbe K 2001 *J. Phys.: Condens. Matter* **13** 6675
[4] Onoda M and Amemiya I 2003 *J. Phys.: Condens. Matter* **15** 3079
[5] de Picciotto L A, Andendorff K T, Liles D C and Thackeray M M 1993 *Solid State Ion.* **62** 297
[6] Casalot A and Pouchard 1967 *Bull. Soc. Chim.* **10** 3817
[7] Wadsley A D 1957 *Acta Crystallogr.* **10** 261
[8] Rozier P and Galy J 1997 *J. Solid State Chem.* **134** 294
[9] Kawakita J, Katayama Y, Miura T and Kishi T 1997 *Solid State Ion.* **99** 71
[10] Kawakita J, Miura T and Kishi T 1999 *Solid State Ion.* **124** 21
[11] Onoda M, Ohta H and Nagasawa H 1991 *Solid State Commun.* **79** 281
[12] Cromer D T and Waber J T 1974 *International Tables for X-Ray Crystallography* vol 4, ed J A Ibers and W C Hamilton (Birmingham: Kynoch) section 2
[13] Creagh D C and McAuley W J 1992 *International Tables for Crystallography* vol C, ed A J C Wilson (Boston, MA: Kluwer–Academic)
[14] teXsan 1992 *Crystal Structure Analysis Package* (The Woodlands, TX: Molecular Structure Corporation)
[15] Shannon R D 1976 *Acta Crystallogr.* A **32** 751
[16] Zachariasen W H 1978 *J. Less-Common Met.* **62** 1
[17] Freeman A J and Watson R E 1965 *Magnetism* part A, vol 2, ed G T Rado and H Suhl (New York: Academic)
[18] See, for example, Goodenough J B 1963 *Magnetism and the Chemical Bond* (New York: Interscience) chapter 3
[19] Efros A L and Shklovskii 1975 *J. Phys. C: Solid State Phys.* **8** L49
[20] Mott N F 1968 *J. Non-Cryst. Solids* **1** 1
[21] Nakhmedov E P, Prigodin V N and Samukhin A N 1989 *Sov. Phys.—Solid State* **31** 368
[22] Brenig W, Döhler G H and Heyszenau H 1973 *Phil. Mag.* **27** 1093
[23] Serota R A, Kalia R K and Lee P A 1986 *Phys. Rev.* B **33** 8441
[24] Kurkijarvi J 1973 *Phys. Rev.* B **8** 922
[25] See, for example, Brenig W, Döhler G H and Wölfle P 1973 *Z. Phys.* **258** 381
[26] Heikes R R 1961 *Thermoelectricity* ed R R Heikes and R W Ure (New York: Interscience)
[27] Usuki T, Kawakami N and Okiji A 1990 *J. Phys. Soc. Japan* **59** 1357
[28] Bonner J C and Fisher M E 1964 *Phys. Rev.* A **3** 640
[29] Onoda M 2002 unpublished results
[30] See, for example, Onoda M and Hasegawa J 2002 *J. Phys.: Condens. Matter* **14** 5045 and references therein